

## UV ray-induced thermoluminescence study of $\text{Y}_2\text{SiO}_5:\text{Ce}^{3+}$ phosphor

Yogita Parganiha<sup>1</sup> · Jagjeet Kaur<sup>1</sup> · Vikas Dubey<sup>2</sup> · Deepika Chandrakar<sup>1</sup> · N. S. Suryanarayana<sup>1</sup>

Received: 7 February 2015 / Accepted: 22 June 2015 / Published online: 1 July 2015  
© Springer Science+Business Media Dordrecht 2015

**Abstract** This paper reports thermoluminescence (TL) properties of  $\text{Ce}^{3+}$  doped yttrium silicate phosphor. The phosphor is synthesized by a solid state reaction method which is suitable for large scale production. Starting materials used for sample preparation were  $\text{Y}_2\text{O}_3$ ,  $\text{SiO}_2$ ,  $\text{CeO}_2$  and a fixed concentration of boric acid used as a flux. The prepared phosphors for different concentrations of  $\text{Ce}^{3+}$  were examined by observing their TL glow curves for UV irradiation (254-nm source). The samples show a well resolved broad peak covering a temperature range of 50–375 °C. The kinetic parameters such as activation energy, order of kinetics and frequency factor were calculated by the peak shape method. Most of the peaks show general order kinetics. The effect of UV exposure on TL was also examined and a linear response to dose was shown, indicating the sample may be useful for a TL dosimeter. The kinetic parameters were calculated using a computerized glow curve de-convolution (CGCD) technique.

**Keywords** Thermoluminescence · UV irradiation · TL dosimeter · Kinetic parameters · CGCD

---

✉ Yogita Parganiha  
parganiha.yogita@rediffmail.com  
Vikas Dubey  
jsvikasdubey@gmail.com

<sup>1</sup> Department of Physics, Govt. Vishwanath Yadav Tamaskar Post Graduate Autonomous College, Durg 491001, C.G., India

<sup>2</sup> Department of Physics, Bhilai Institute of Technology, Kendri, Raipur, C.G., India

## Introduction

Thermoluminescence (TL) is the thermally stimulated emission of light following the previous absorption of energy from radiation like  $\alpha$ ,  $\beta$ ,  $\gamma$ , X-rays or ultraviolet (UV) rays. There are three essential conditions necessary for production of TL. Firstly, the material must be an insulator or semiconductor; metals do not exhibit luminescent properties. Secondly, the material must have at some time absorbed energy during exposure to radiation. Thirdly, the luminescence emission is triggered by heating the material. It is the characteristics of TL that, once heated to excite the light emission, the material cannot be made to emit TL again by simply cooling the material and reheating. In order to re-exhibit the luminescence, the material has to be re-exposed to radiation. The normal way of displaying TL data is to plot luminescence intensity as a function of temperature, known as a 'glow curve' [1]. The relationship between irradiation dose and TL intensity enables potential application of the sample in dosimetry [2, 3]. TL dosimetry has been an active field for environmental and personal radiation monitoring. It has been found that the intensity and area of TL glow peaks are proportional to the received dose and this has been the basis for dosimetry of ionizing radiations by TL phosphors. The intensity of light emitted during heating by a sample gives an idea about the radiation dose given to it and the concentration of defect centers caused by the interaction of ionizing radiation with the matter comprising the sample [4–6]. TL is used in diverse fields such as dosimetry, geology, biology, archaeology, biochemistry, space science, forensic science, TSL photography, radiation physics and so on.

The TL glow curve is related to the trap levels lying at different depths in the band gap between the conduction and the valence bands of a solid. These trap levels are characterized by different trapping parameters such as trap depth, order of kinetics, and frequency factor [7]. The loss of dosimetry information stored in the materials after irradiation is strongly dependent on the position of trapping levels within the forbidden gap, which is known as trap depth or activation energy ( $E$ ). The mechanism of recombining de-trapped charge carriers with their counterparts is known as the order of kinetics ( $b$ ). The frequency factor ( $s$ ) represents the product of the number of times an electron hits the wall and the wall reflection coefficient, treating the trap as a potential well. Thus, a reliable dosimetry study of thermoluminescent material is based on its trapping parameters [8].

$Y_2SiO_5$  is a well known luminescent material. It is used in positron emission tomography (PET). TL studies of  $Y_2SiO_5$  single-crystal and single-crystal film after  $\alpha$  and  $\beta$  irradiation [9], and  $Y_2SiO_5$  phosphor (YSO) crystal after X-ray irradiation [10, 11] have been done by many researchers.

The present study shows the effect of  $Ce^{3+}$  concentration on the TL properties of  $Y_2SiO_5$  phosphor (YSO) synthesized by solid state reaction method. The TL glow curves show a single peak for UV radiation. The effect of different UV exposure times for different  $Ce^{3+}$  concentration  $Y_2SiO_5$  was interpreted. The effect of heating rate on TL was studied and trapping parameter calculations were interpreted by the peak shape method. Manuscript gives the important factor for UV dosimetric applications in silicate-based phosphor. The effect of cerium ion concentration and

the calculation of kinetic parameters provides information about dosimetric loss in the prepared phosphor.

## Solid state synthesis of $\text{Y}_2\text{SiO}_5:\text{Ce}^{3+}$ phosphor

For synthesis of samples via solid state reaction method,  $\text{Y}_2\text{O}_3$ ,  $\text{SiO}_2$  and  $\text{CeO}_2$  were mixed in a stoichiometric ratio by dry grinding in mortar and pestle for nearly 45 min. The mixture was taken in alumina crucible and fired in air at 1000 °C for 1 h, followed by dry grinding and further heated at 1400 °C for 3 h in a muffle furnace in the presence of boric acid ( $\text{H}_3\text{BO}_3$ ) as a flux. The concentration of  $\text{Ce}^{3+}$  ions were 0.1–2.5 mol% [12].

Crystalline phases and sizes of prepared phosphors were characterized by X-ray powder diffraction (XRD) carried out using a Bruker D8 Advance X-ray diffractometer. The X-rays were produced by a sealed tube and the wavelength of X-ray was 0.154 nm ( $\text{Cu K}\alpha$ ). The X-rays were detected using a fast-counting, detector based on silicon strip technology. Fourier transform infrared (FTIR) analysis was carried out at room temperature in the wave number range of 4000–400  $\text{cm}^{-1}$  on a Bruker spectrophotometer (Germany). For measurement of FTIR spectra, the sample was mixed with a mulling agent, like mineral oil, and pressed between plates of potassium bromide because it is transparent to 400  $\text{cm}^{-1}$ . The size of the crystallite was calculated by using Scherer's formula. The obtained phosphor under the TL examination is given UV radiation using a 254-nm UV source TL glow curves were recorded at room temperature using a TLD reader I1009 supplied by Nucleonix Sys. Pvt. Ltd. Hyderabad [13–16].

## Characterization of prepared phosphor

### XRD of $\text{Y}_2\text{SiO}_5:\text{Ce}^{3+}$ phosphor

Figure 1 shows the XRD pattern of  $\text{Y}_2\text{SiO}_5:\text{Ce}^{3+}$  phosphor for variable concentrations of  $\text{Ce}^{3+}$  (0.1, 1, 1.5, 2 and 2.5 mol%). From the XRD pattern, there is no considerable change in the peak position with the doping concentration of  $\text{Ce}^{3+}$  and in the final crystallite size of the phosphor, the peak index revealed the monoclinic phase of  $\text{Y}_2\text{SiO}_5$ . They are in good accordance with JCPDS card no. 36-1476. It is indicated that there is no other impurity phase that can be observed in the phosphor sample. From these experimental results, we can conclude that  $\text{Ce}^{3+}$  ions have been introduced into the  $\text{Y}_2\text{SiO}_5$  lattice, and do not cause any change in the monoclinic structure. Any effect of flux ( $\text{H}_3\text{BO}_3$ ) was not found in the XRD patterns. The size of the crystal was computed from the full width half maximum (FWHM) of every peak using Scherer's formula [17]. The crystallite size calculated by Scherer's formula is presented in Table 1. It confirms the formation of nano-crystallites in phosphor  $\text{Y}_2\text{SiO}_5:\text{Ce}^{3+}$ .

Additional details regarding the particle size distribution and morphology of the prepared phosphor were provided by scanning electron microscopy (SEM) and field emission gun scanning electron microscopy (FEGSEM).

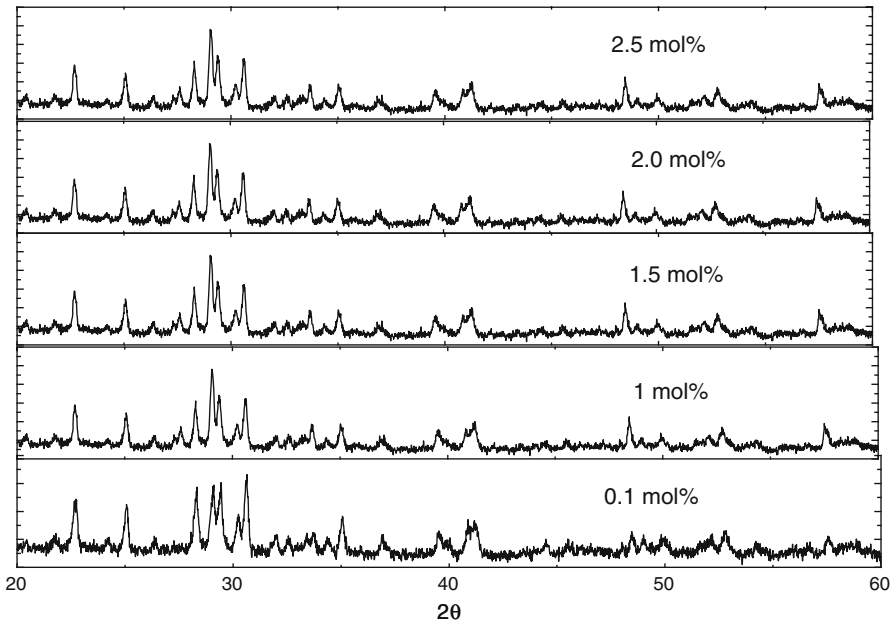


**Fig. 1** XRD pattern of  $\text{Y}_2\text{SiO}_5:\text{Ce}^{3+}$

**Table 1** Crystallite size calculation of  $\text{Y}_2\text{SiO}_5:\text{Ce}^{3+}$  using its XRD pattern

S. No	$2\theta$	FWHM	h k l	$D$ crystallite size (nm)
1	22.91	0.18	211	42
2	24.99	0.20	112	40
3	29.11	0.25	013	34
4	30.66	0.32	402	23
5	33.56	0.12	312	50
6	35.08	0.23	411	38
7	39.37	0.15	420	44.5
8	41.17	0.31	031	24.6
9	48.64	0.40	314	20
10	50.16	0.34	431	22
11	52.78	0.34	622	22
12	57.34	0.32	042	23

Prepared phosphor was characterized by SEM and FEGSEM images, and it was found that the particle sizes were distributed between nanometers to a few microns, with a compact distribution and a clustered-like structure (Fig. 2a, b).

### FTIR analysis of $\text{Y}_2\text{SiO}_5:\text{Ce}^{3+}$

Figure 3 shows FTIR spectra of the sample. In the spectrum, the absorption band of silicate groups are clearly evident. The intense broad band from  $909$  to  $1100\text{ cm}^{-1}$

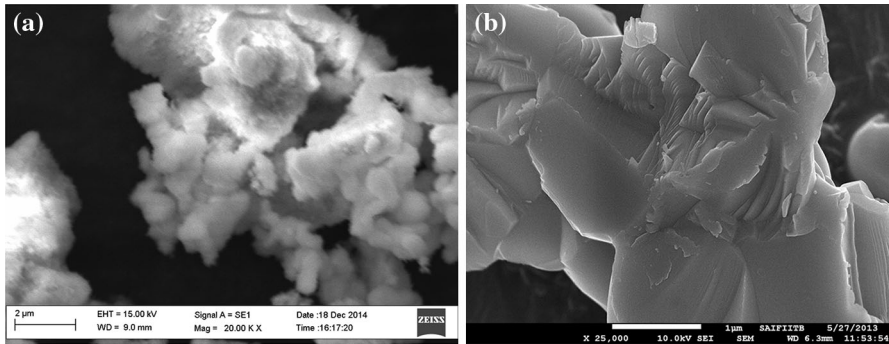


**Fig. 2** (a) SEM and (b) FEGSEM micrographs of prepared phosphor



**Fig. 3** FTIR spectra of  $Y_2SiO_5:Ce^{3+}$

is assigned to the presence of a  $SiO_4^{2-}$  group. The bands at 408, 420, 427, 444, 458, 478, 483 and  $489\text{ cm}^{-1}$  are assigned to the Si–O–Si vibrational mode of bending. The band at  $552\text{ cm}^{-1}$  is due to bending vibration of Y–O bonds. The peaks at 687 and  $718\text{ cm}^{-1}$  are assigned to Ce–O vibration. Two small peaks originated at 2365 and  $2924\text{ cm}^{-1}$  are due to filter contamination of the FTIR instrument.

## TL studies

Kinetic parameters such as trap depth ( $E$ ) which is the loss of dosimetry information stored in the materials after irradiation, order of kinetics ( $b$ ), which is the mechanism of recombination of detrapped charge carriers with their counter parts,

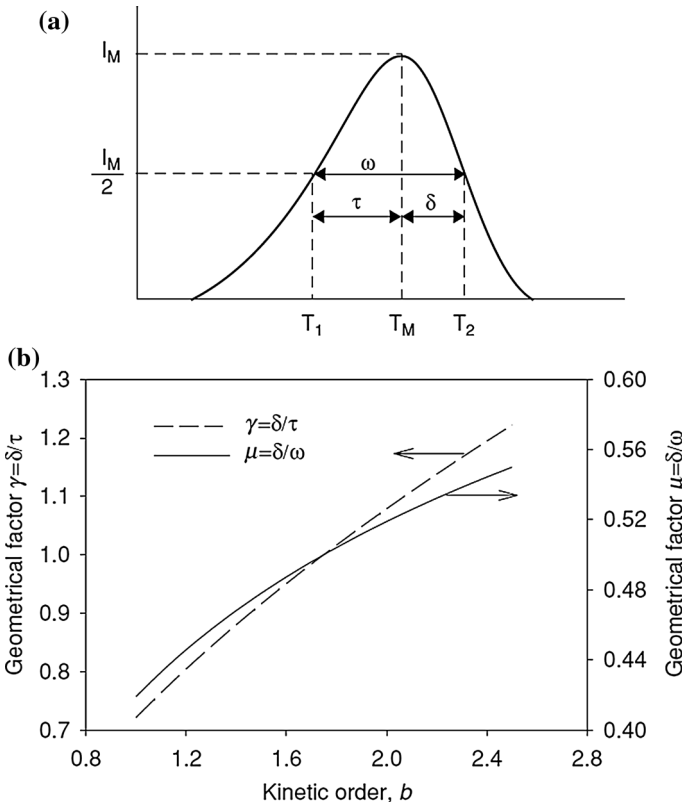


**Fig. 4** **a** Representation of shape factors  $\tau$ ,  $\delta$ , and  $\omega$  [1]. **b** Graph between the kinetic order (**b**) and the geometrical factor [1]

and the frequency factor ( $s$ ), which represents the product of the number of times an electron hits the wall and the wall reflection coefficient, treating the trap as a potential well for the glow curves, which were obtained after UV excitation. The estimation of trap depth ( $E$ ) was done by applying Chen’s peak shape method with Eq. (1).

$$E_\alpha = c_\alpha(kT_M^2/\alpha) - b_\alpha(2kT_M) \tag{1}$$

where  $k$  = Boltzmann constant.  $\alpha = \tau, \delta, \omega$ . The values of  $c_\alpha$  and  $b_\alpha$  are summarized as below:

$$c_\tau = 1.510 + 3.0(\mu - 0.42) \quad b_\tau = 1.58 + 4.2(\mu - 0.42)$$

$$c_\delta = 0.976 + 7.3(\mu - 0.42) \quad b_\delta = 0$$

$$c_\omega = 2.52 + 10.2(\mu - 0.42) \quad b_\omega = 1$$

The relationship between the frequency factor ( $s$ ) and the trap depth ( $E$ ) is given by the following equation:

$$\beta E/kT_M^2 = \text{sexp}(-E/kT_M) [1 + (b - 1)(2kT_M/E)] \tag{2}$$

In Fig. 4a,  $T_1, T_2$  = temperatures on either side of  $T_M$ , corresponding to half intensity

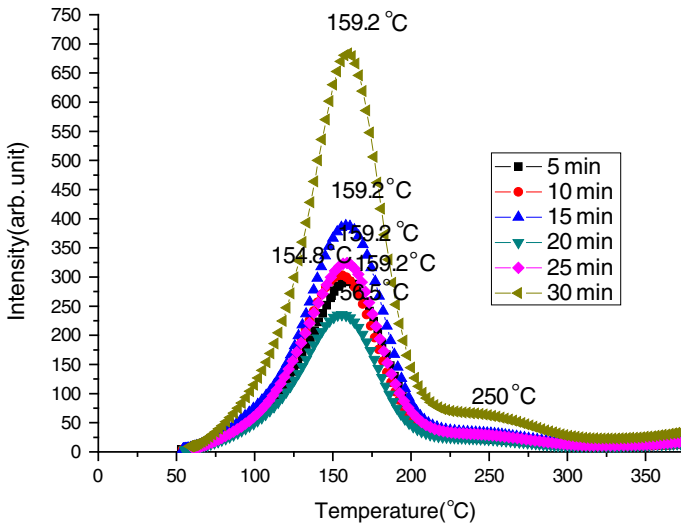
$$\tau = T_M - T_1, \delta = T_2 - T_M, \omega = T_2 - T_1 \text{ and } \mu = \delta/\omega.$$

The value of order of kinetics ( $b$ ) may be estimated by the value of the shape factor ( $\mu$ ) using the following graph (Fig. 4b) [18].

**TL studies for different UV exposure time**

Figure 5 shows the TL glow curve of  $Y_2SiO_5$  doped with 0.1 mol%  $Ce^{3+}$  for different UV exposure times at a constant heating rate (i.e.,  $5^\circ C s^{-1}$ ). The sample show peaks at 159.2, 154.8, 159.2, 156.5, 159.2 and 159.2  $^\circ C$  for 5, 10, 15, 20, 25 and 30-min UV exposure time, respectively, and shows general order kinetics. The TL intensity increases up to 20 min of UV dose, then it decreases. Table 2 shows the effect of different UV exposure times on the peak temperature of the phosphor. To estimate the order of kinetics, the shape factor was calculated by the peak shape method [8, 15, 16]. For  $Y_2SiO_5$  doped with 0.1 mol%  $Ce^{3+}$ , the frequency factor found between  $1.8 \times 10^6$  and  $6.5 \times 10^8$ . Trap depth was also calculated, which was found to be in the range from 0.67–0.80 eV.

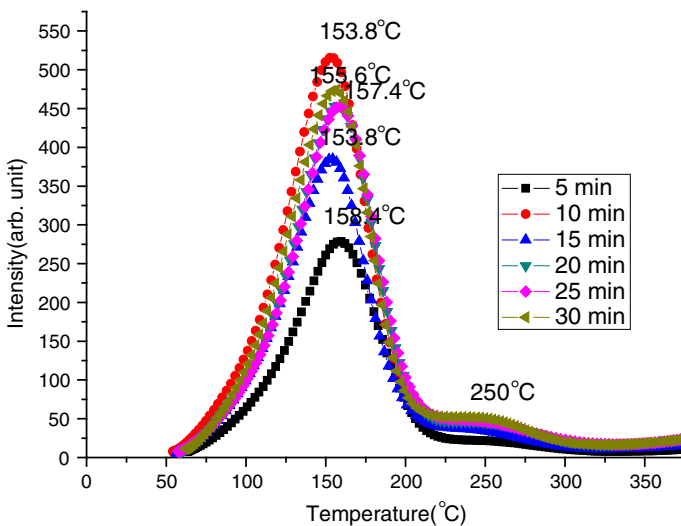
Figure 6 shows the TL glow curve of  $Y_2SiO_5$  doped with 0.2 mol%  $Ce^{3+}$  with different UV exposure times at a constant heating rate (i.e.  $5^\circ C s^{-1}$ ). The sample



**Fig. 5** TL glow curve of  $Y_2SiO_5:Ce^{3+}$  (0.1 %) for different UV exposure times with a heating rate of  $5^\circ C s^{-1}$

**Table 2** Shape factor ( $\mu$ ), activation energy ( $E$ ), and frequency factor ( $s$ ) for UV-irradiated  $Y_2SiO_5:Ce(0.1\%)$  phosphor

UV exposure (min)	$T_1$	$T_m$	$T_2$	$\tau$	$\delta$	$\omega$	$\mu = \delta/\omega$	Activation energy ( $E$ )	Frequency factor ( $s$ )
5	126.7	159.2	187.2	32.5	28.0	60.5	0.46	0.70	$3.3 \times 10^7$
10	123.1	154.8	182.7	31.7	27.9	59.6	0.47	0.72	$7.9 \times 10^7$
15	128.4	159.2	187.3	30.8	28.1	58.9	0.48	0.77	$2.8 \times 10^8$
20	123.9	156.5	183.6	32.6	27.1	59.7	0.45	0.67	$1.8 \times 10^7$
25	124.8	159.2	184.6	34.4	25.4	59.8	0.42	0.60	$1.8 \times 10^6$
30	129.4	159.2	186.3	29.8	27.1	56.9	0.48	0.80	$6.5 \times 10^8$

**Fig. 6** TL glow curve of  $Y_2SiO_5:Ce^{3+}$  (0.2%) for different UV exposure times with a heating rate of  $5\text{ }^\circ\text{C s}^{-1}$ 

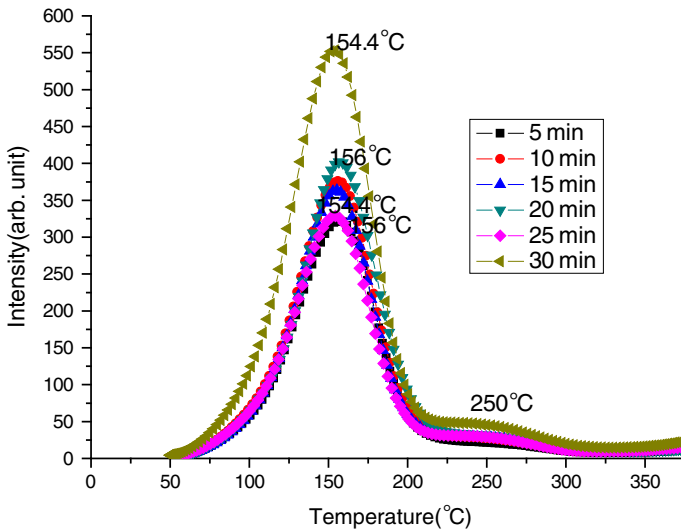
shows peaks at 158.4, 153.8, 153.8, 157.4, 157.4 and 155.6  $^\circ\text{C}$  for 5, 10, 15, 20, 25 and 30-min UV exposure times, respectively, and shows general order kinetics. The TL intensity increases up to 10 min of UV dose, then it decreases. Table 3 shows the effects of different UV exposures time on peak temperature of the phosphor. For  $Y_2SiO_5$  doped with 0.2 mol%  $Ce^{3+}$ , the frequency factor lies between  $2.5 \times 10^6$  and  $2.8 \times 10^7$ . Trap depth was also calculated and was found to be in the range of 0.61–0.69 eV.

Figure 7 shows the TL glow curve of  $Y_2SiO_5$  doped with 0.5 mol%  $Ce^{3+}$  with different UV exposure times at a constant heating rate (i.e.  $5\text{ }^\circ\text{C s}^{-1}$ ). The sample shows peaks at 156.0, 156.0, 156.0, 156.0, 154.4 and 154.0  $^\circ\text{C}$  for 5, 10, 15, 20, 25 and 30-min UV exposure times, respectively, and shows general order kinetics. The TL intensity increases up to 20 min of UV dose, then it decreases. Table 4 shows



**Table 3** Shape factor ( $\mu$ ), activation energy ( $E$ ), and frequency factor ( $s$ ) for UV-irradiated  $Y_2SiO_5:Ce(0.2\%)$  phosphor

UV exposure (min)	$T_1$	$T_m$	$T_2$	$\tau$	$\delta$	$\omega$	$\mu = \delta/\omega$	Activation energy ( $E$ )	Frequency factor ( $s$ )
5	124.8	158.4	187.2	33.6	28.8	62.4	0.46	0.67	$1.6 \times 10^7$
10	119.5	153.8	180.9	34.3	27.1	61.4	0.44	0.62	$4.3 \times 10^6$
15	119.5	153.8	180.0	34.3	26.2	60.5	0.43	0.60	$2.7 \times 10^6$
20	124.8	157.4	185.5	32.6	28.1	60.7	0.46	0.69	$2.8 \times 10^7$
25	124.8	157.4	185.5	32.6	28.1	60.7	0.46	0.69	$2.8 \times 10^7$
30	120.3	155.6	186.6	35.3	28.0	63.3	0.44	0.61	$2.5 \times 10^6$



**Fig. 7** TL glow curve of  $Y_2SiO_5:Ce^{3+}$  (0.5 %) for different UV exposure times with a heating rate of  $5^\circ C s^{-1}$

**Table 4** Shape factor ( $\mu$ ), activation energy ( $E$ ), and frequency factor ( $s$ ) for UV-irradiated  $Y_2SiO_5:Ce(0.5\%)$  phosphor

UV exposure (min)	$T_1$	$T_m$	$T_2$	$\tau$	$\delta$	$\omega$	$\mu = \delta/\omega$	Activation energy ( $E$ )	Frequency factor ( $s$ )
5	123.9	156.0	183.6	32.1	27.6	59.7	0.46	0.70	$3.5 \times 10^7$
10	126.7	156.0	181.9	29.3	25.9	55.2	0.47	0.79	$4.5 \times 10^8$
15	125.8	156.0	180.9	30.2	24.9	55.1	0.45	0.73	$8.4 \times 10^7$
20	127.5	156.0	186.0	28.5	30.0	58.5	0.51	0.85	$2.4 \times 10^9$
25	123.9	154.4	180.9	30.5	26.5	57.0	0.46	0.73	$9.0 \times 10^7$
30	121.2	154.4	181.9	33.2	27.5	60.7	0.45	0.65	$1.1 \times 10^7$

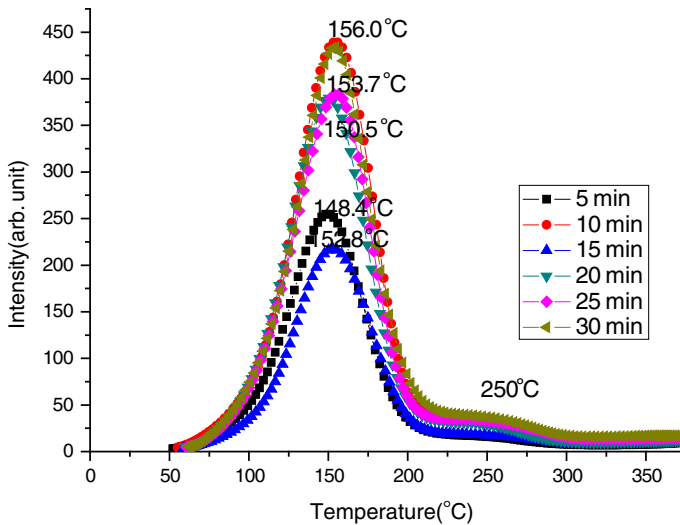


**Fig. 8** TL glow curve of  $\text{Y}_2\text{SiO}_5:\text{Ce}^{3+}$  (1 %) for different UV exposure times with a heating rate of  $5^\circ\text{C s}^{-1}$

**Table 5** Shape factor ( $\mu$ ), activation energy ( $E$ ), and frequency factor ( $s$ ) for UV-irradiated  $\text{Y}_2\text{SiO}_5:\text{Ce}$  (1 %) phosphor

UV exposure (min)	$T_1$	$T_m$	$T_2$	$\tau$	$\delta$	$\omega$	$\mu = \delta/\omega$	Activation energy ( $E$ )	Frequency factor ( $s$ )
5	121.4	148.4	177.3	27.20	28.90	56.10	0.52	0.89	$8.9 \times 10^9$
10	126.7	156.0	182.7	29.30	26.70	56.00	0.48	0.81	$8.0 \times 10^8$
15	124.8	152.8	180.9	28.0	28.10	56.10	0.52	0.91	$1.5 \times 10^{10}$
20	122.2	150.5	178.3	28.30	27.80	56.10	0.50	0.87	$5.9 \times 10^9$
25	123.1	153.7	181.9	30.60	28.20	58.80	0.48	0.76	$2.1 \times 10^8$
30	124.8	156.0	180.9	31.20	24.90	56.10	0.44	0.69	$3.1 \times 10^7$

the effect of different UV exposures on the peak temperature of the phosphor TL glow curve. For  $\text{Y}_2\text{SiO}_5$  doped with 0.5 mol%  $\text{Ce}^{3+}$ , the frequency factor found between  $1.1 \times 10^7$  and  $2.4 \times 10^9$ . Trap depth was also calculated and it is in the range of 0.65–0.85 eV.

Figure 8 shows the TL glow curve of  $\text{Y}_2\text{SiO}_5$  doped with 1 mol%  $\text{Ce}^{3+}$  with different UV exposure times at a constant heating rate (i.e.  $5^\circ\text{C s}^{-1}$ ). The sample shows peaks at 148.4, 156.0, 152.8, 150.5, 153.7 and 156.0  $^\circ\text{C}$  for 5, 10, 15, 20, 25 and 30-min UV exposure times, respectively, and shows general order kinetics. The TL intensity increases up to 10 min of UV dose, then it decreases. Table 5 shows the effect of varying UV exposure on the peak temperature of the phosphor. For  $\text{Y}_2\text{SiO}_5$  doped with 1 mol%  $\text{Ce}^{3+}$ , the frequency factor is between  $3.1 \times 10^7$  and  $1.5 \times 10^{10}$ . Trap depth was also calculated and it is in the range of 0.69–0.91 eV.

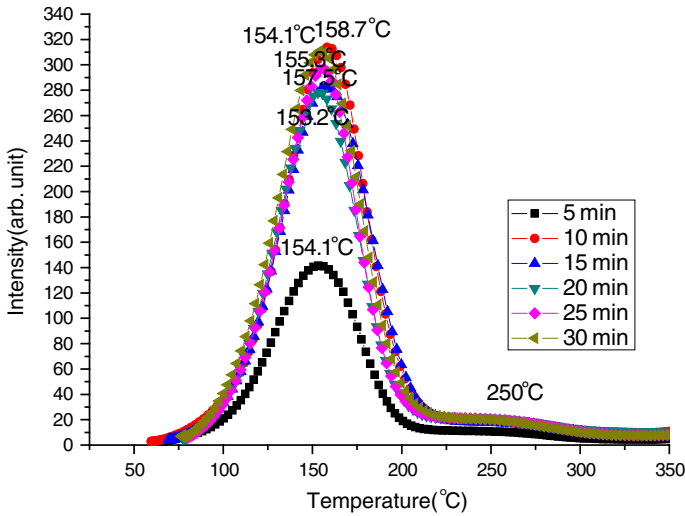


**Fig. 9** TL glow curve of  $Y_2SiO_5:Ce^{3+}$  (1.5 %) for different UV exposure times with a heating rate of  $5\text{ }^\circ\text{C s}^{-1}$

**Table 6** Shape factor ( $\mu$ ), activation energy ( $E$ ), and frequency factor ( $s$ ) for UV-irradiated  $Y_2SiO_5:Ce(1.5\text{ } \%)$  phosphor

UV exposure (min)	$T_1$	$T_m$	$T_2$	$\tau$	$\delta$	$\omega$	$\mu = \delta/\omega$	Activation energy ( $E$ )	Frequency factor ( $s$ )
5	123.9	154.1	180.3	30.2	26.2	56.4	0.46	0.74	$1.2 \times 10^8$
10	129.3	158.7	184.6	29.4	25.9	55.3	0.47	0.80	$5.2 \times 10^8$
15	126.9	157.5	186.9	30.6	29.4	60.0	0.49	0.78	$3.1 \times 10^8$
20	125.9	153.2	183.5	27.3	30.3	57.6	0.53	0.91	$1.5 \times 10^{10}$
25	127.1	155.3	179.1	28.2	23.8	52.0	0.46	0.81	$8.4 \times 10^8$
30	125.9	154.1	180.3	28.2	26.2	54.4	0.48	0.82	$1.1 \times 10^9$

Figure 9 shows the TL glow curve of  $Y_2SiO_5$  doped with 1.5 mol%  $Ce^{3+}$  with different UV exposure times at a constant heating rate (i.e.  $5\text{ }^\circ\text{C s}^{-1}$ ). The sample shows peaks at 154.1, 158.7, 157.5, 153.2, 155.3 and 154.1  $^\circ\text{C}$  for 5, 10, 15, 20, 25 and 30-min UV exposure times, respectively, and shows general order kinetics. The TL intensity increases up to 10 min of UV dose, then it decreases. Table 6 shows the effect of different UV exposures on the peak temperature of phosphor. For  $Y_2SiO_5$  doped with 1.5 mol%  $Ce^{3+}$ , the frequency factor ranges from  $1.2 \times 10^8$  to  $1.5 \times 10^{10}$ . Trap depth was also calculated and was found to be in the range 0.74–0.91 eV.

Figure 10 shows the TL glow curve of  $Y_2SiO_5$  doped with 2 mol%  $Ce^{3+}$  with different UV exposure times at a constant heating rate (i.e.  $5\text{ }^\circ\text{C s}^{-1}$ ). The sample shows peaks at 145.2, 152.8, 152.8, 154.5, 154.5 and 157.0  $^\circ\text{C}$  for 5, 10, 15, 20, 25 and 30-min UV exposure times, respectively, and shows general order kinetics. The

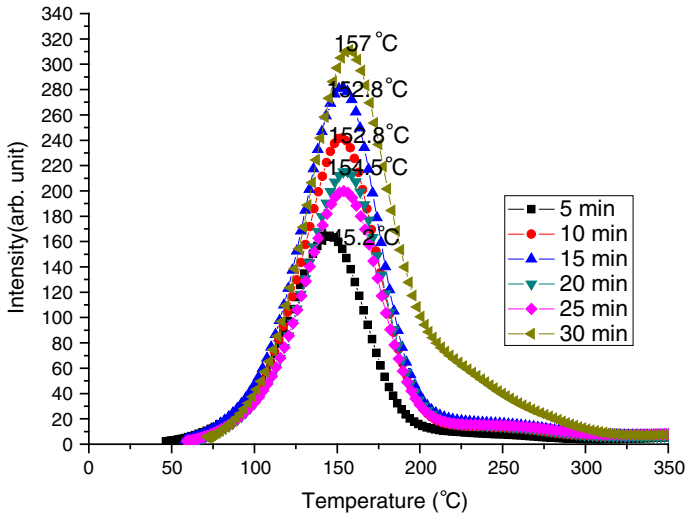


**Fig. 10** TL glow curve of  $\text{Y}_2\text{SiO}_5:\text{Ce}^{3+}$  (2%) for different UV exposure times with a heating rate of  $5^\circ\text{C s}^{-1}$

**Table 7** Shape factor ( $\mu$ ), activation energy ( $E$ ), and frequency factor ( $s$ ) for UV-irradiated  $\text{Y}_2\text{SiO}_5:\text{Ce}$  (2%) phosphor

UV exposure (min)	$T_1$	$T_m$	$T_2$	$\tau$	$\delta$	$\omega$	$\mu = \delta/\omega$	Activation energy ( $E$ )	Frequency factor ( $s$ )
5	114.9	145.2	171.4	30.3	26.2	56.5	0.46	0.74	$1.9 \times 10^9$
10	124.1	152.8	179	28.7	26.2	54.9	0.48	0.83	$1.6 \times 10^9$
15	124.1	152.8	179	28.7	26.2	54.9	0.48	0.83	$1.6 \times 10^9$
20	125.9	154.5	181.5	28.6	27	55.6	0.49	0.83	$1.5 \times 10^9$
25	124.1	154.5	181.5	30.4	27	57.4	0.47	0.75	$1.5 \times 10^9$
30	126.6	157.0	188.3	30.4	31.3	61.7	0.51	0.81	$1.3 \times 10^9$

TL intensity increases up to 10 min of UV dose, then it decreases. Table 7 shows the effect of different UV exposure time on the peak temperature of the phosphor. For  $\text{Y}_2\text{SiO}_5$  doped with 1.5 mol%  $\text{Ce}^{3+}$ , the frequency factor ranges between  $1.3 \times 10^9$  and  $1.9 \times 10^9$ . Trap depth was also calculated and was found to be in the range 0.74–0.83 eV.

Figure 11 shows the TL glow curve of  $\text{Y}_2\text{SiO}_5$  doped with 2.5 mol%  $\text{Ce}^{3+}$  with different UV exposure times at a constant heating rate (i.e.  $5^\circ\text{C s}^{-1}$ ). The sample shows peaks at 149.4, 152.8, 153.7, 157.9, 151.2 and 153.7  $^\circ\text{C}$  for 5, 10, 15, 20, 25 and 30-min UV exposure times, respectively, and shows general order kinetics. The TL intensity increases up to 15 min of UV dose, then it decreases. Table 8 shows the effect of different UV exposure time on the peak temperature of the phosphor. For  $\text{Y}_2\text{SiO}_5$  doped with 1.5 mol%  $\text{Ce}^{3+}$ , the frequency factor ranges between  $1.0 \times 10^8$  and  $5.2 \times 10^9$ . Trap depth was also calculated and was found to be in the range 0.74–0.87 eV.

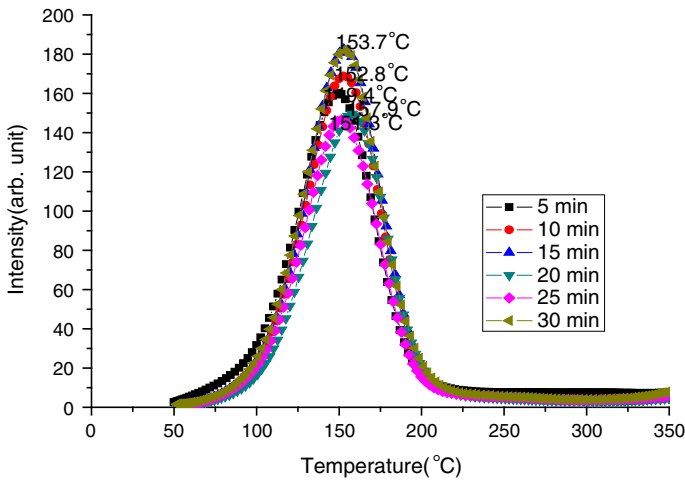


**Fig. 11** TL glow curve of  $Y_2SiO_5:Ce^{3+}$  (2.5 %) for different UV exposure times with a heating rate of  $5\text{ }^\circ\text{C s}^{-1}$

**Table 8** Shape factor ( $\mu$ ), activation energy ( $E$ ), and frequency factor ( $s$ ) for UV-irradiated  $Y_2SiO_5:Ce(2.5\text{ \%})$  phosphor

UV exposure (min)	$T_1$	$T_m$	$T_2$	$\tau$	$\delta$	$\omega$	$\mu = \delta/\omega$	Activation energy ( $E$ )	Frequency factor ( $s$ )
5	120.8	149.4	175.6	28.6	26.2	54.8	0.48	0.82	$1.5 \times 10^9$
10	125.0	152.8	179.8	27.8	27	54.8	0.49	0.87	$5.2 \times 10^9$
15	124.1	153.7	178.1	29.6	24.4	54	0.45	0.75	$1.6 \times 10^8$
20	128.4	157.9	181.5	29.5	23.6	53.1	0.44	0.74	$1.0 \times 10^8$
25	124.1	151.2	177.4	27.1	26.2	53.3	0.49	0.86	$4.3 \times 10^9$
30	124.1	153.7	178.1	29.6	24.4	54	0.45	0.86	$4.3 \times 10^9$

**Concentration effect on TL glow curve**

Figure 12 shows the TL glow curve of  $Y_2SiO_5$  doped with variable concentrations of  $Ce^{3+}$  (0.1–2.5 %) for fixed UV exposure times (i.e., 10 min at a constant heating rate of  $5\text{ }^\circ\text{C s}^{-1}$ ). The sample shows general order kinetics. The TL intensity increases up to 0.2 %  $Ce^{3+}$  concentration, then it decreases. Table 9 shows the effect of different  $Ce^{3+}$  concentrations on the peak temperature of the phosphor. For  $Y_2SiO_5$  doped with variable  $Ce^{3+}$ , concentration frequency factor ranges between  $4.3 \times 10^6$  and  $5.2 \times 10^9$ . Trap depth was also calculated, and was found to be in the range 0.62–0.87 eV.

The decrease in TL glow curve intensity is due to the  $Ce^{3+}$  ion increases; ion—ion interaction between the host and dopant occurs and, due to this phenomenon, the peak intensity of the TL glow curve decreases. This is known as concentration quenching.

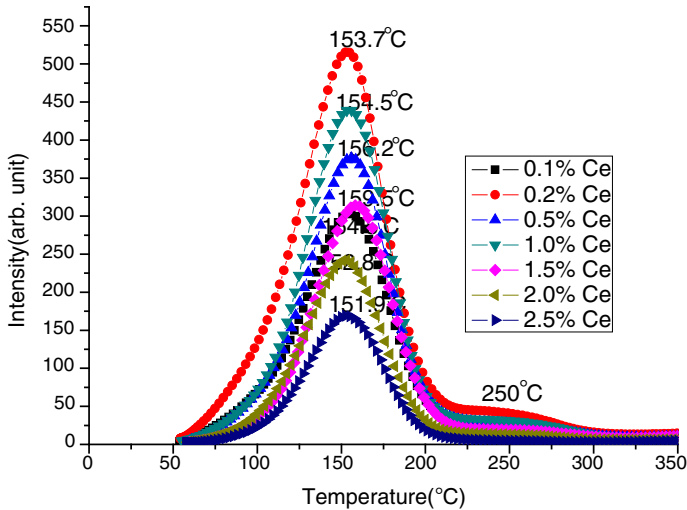


**Fig. 12** TL glow curve of  $\text{Y}_2\text{SiO}_5:\text{Ce}^{3+}$  for variable  $\text{Ce}^{3+}$  concentrations (0.1–2.5 %) with a heating rate of  $5\text{ }^\circ\text{C s}^{-1}$

**Table 9** Shape factor ( $\mu$ ), activation energy ( $E$ ), and frequency factor ( $s$ ) for 10 min UV-irradiated  $\text{Y}_2\text{SiO}_5:\text{Ce}^{3+}$  phosphor with variable  $\text{Ce}^{3+}$  concentrations

$\text{Ce}^{3+}$ concentration (%)	$T_1$	$T_m$	$T_2$	$\tau$	$\delta$	$\omega$	$\mu = \delta/\omega$	Activation energy ( $E$ )	Frequency factor ( $s$ )
0.1	123.1	154.8	182.7	31.7	27.9	59.6	0.47	0.72	$7.9 \times 10^7$
0.2	119.5	153.8	180.9	34.3	27.1	61.4	0.44	0.62	$4.3 \times 10^6$
0.5	126.7	156.0	181.9	29.3	25.9	55.2	0.47	0.79	$4.5 \times 10^8$
1.0	126.7	156.0	182.7	29.3	26.7	56.0	0.48	0.81	$8.0 \times 10^8$
1.5	129.3	158.7	184.6	29.4	25.9	55.3	0.47	0.80	$5.2 \times 10^8$
2.0	124.1	152.8	178.1	28.7	25.3	54.0	0.47	0.80	$7.2 \times 10^7$
2.5	125.0	152.8	179.8	27.8	27.0	54.8	0.49	0.87	$5.2 \times 10^9$

### Heating rate effect

Figure 13 shows the TL glow curve of  $\text{Y}_2\text{SiO}_5$  doped with of  $\text{Ce}^{3+}$  (0.2 %) for a fixed UV exposure time (i.e. 10 min) at variable heating rates. The sample shows general order kinetics. As the heating rate increases, the TL peak shift towards higher temperature side and intensity decreases; it might be due to the thermal quenching of TL due to an increase in heating rate [14]. Table 10 shows the effect of different heating rates on peak temperature of the phosphor TL glow curve. For  $\text{Y}_2\text{SiO}_5$  doped with 0.2 %  $\text{Ce}^{3+}$ , concentration frequency factor ranges between  $3.3 \times 10^5$  and  $4.5 \times 10^7$ . Trap depth was also calculated and was found to be in the range 0.54–0.71 eV.

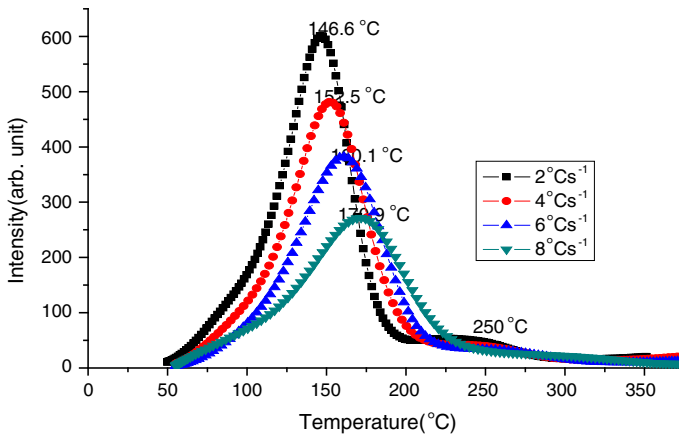


**Fig. 13** TL glow curve of  $Y_2SiO_5:Ce^{3+}$  (0.2 %) for 10-min UV dose with variable heating rates

**Table 10** Shape factor ( $\mu$ ), activation energy ( $E$ ), and frequency factor ( $s$ ) for 10-min UV-irradiated  $Y_2SiO_5:Ce^{3+}$  (0.2 %) phosphor with variable heating rates

Heating rate ( $^{\circ}C\ s^{-1}$ )	$T_1$	$T_m$	$T_2$	$\tau$	$\delta$	$\omega$	$\mu = \delta/\omega$	Activation energy ( $E$ )	Frequency factor ( $s$ )
2	117.1	146.6	168.6	29.5	22.0	51.5	0.43	0.69	$1.7 \times 10^7$
4	121.3	152.5	178.7	31.5	26.2	57.4	0.46	0.71	$4.5 \times 10^7$
6	125.4	160.1	190.5	34.7	30.4	65.1	0.47	0.67	$1.4 \times 10^7$
8	128.4	170.9	205.4	42.5	34.5	77.0	0.45	0.54	$3.3 \times 10^5$

### Computerised glow curve deconvolution (CGCD) analysis

TLD phosphor generally exhibits one or more peaks when the charge carries (holes or electrons) were released. The dosimetric properties of TL materials largely depend on the kinetic parameters ( $E$ ,  $b$  and  $s$ ). These parameters will give valuable information about the mechanism responsible for the emission in the phosphor. For good TLD phosphor, a clear knowledge of its kinetic parameters is highly essential. These parameters can be estimated using Chen's set of empirical equations. For the peak shape method, by deconvoluting the glow curve using glow curve deconvolution (Fig. 14). The peak shape method was generally called Chen's peak method which was used to determine the kinetic parameters of the glow peak of the TL materials (Table 11).

The estimated kinetic parameters for  $Y_2SiO_5:Ce^{3+}$  phosphor is calculated by curve fitting techniques applied to the CGCD curve of the experimental data and the peak shape method proposed by Chen and others. Here, three distinct peaks were found and the shoulder peak at 250  $^{\circ}C$  was easily determined by this technique. Kinetic parameters were easily described for higher temperature peaks and all peaks were fitted easily. Activation energy was found in the range 0.54–0.81 eV and order of kinetics was found to be in the first order.

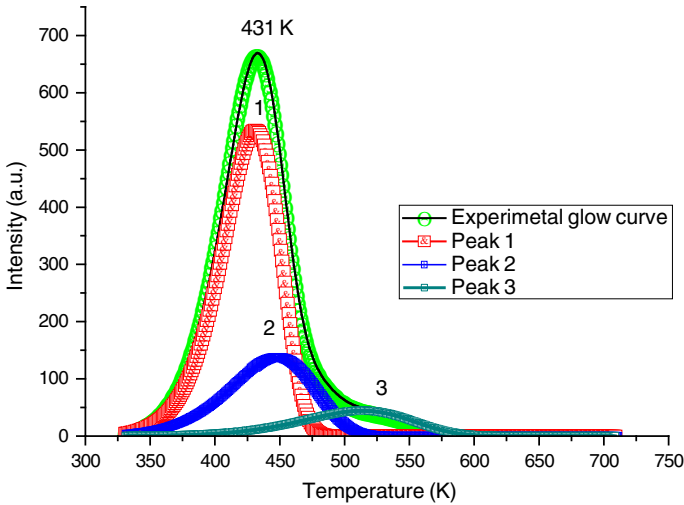
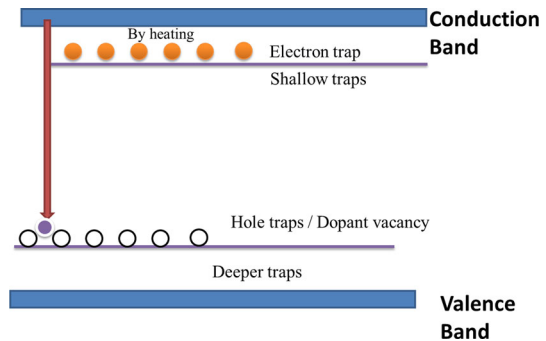


**Fig. 14** CGCD curve of experimental TL glow peak

**Table 11** Typical trapping parameters of the deconvoluted peaks

Peak	$T_1$	$T_m$	$T_2$	$\tau$	$\delta$	$\omega$	$\mu = \delta/\omega$	Activation energy ( $E$ )	Frequency factor ( $s$ )
Peak 1	129	158	179	29	21	50	0.42	0.81	$5 \times 10^{10}$
Peak 2	127	173	208	46	35	81	0.43	0.54	$1 \times 10^7$
Peak 3	194	250	291	56	41	97	0.42	0.61	$6 \times 10^6$

**Fig. 15** Trap model for UV-irradiated  $Y_2SiO_5:Ce^{3+}$  phosphor



**Discussion and model for UV-irradiated phosphor**

We present a model to explain the TL response of  $Y_2SiO_5:Ce^{3+}$  phosphor to UV radiation. In existing model, irradiation of a sample with an electron beam creates two types of trap, one shallower and the other deeper, in the forbidden band gap of the material (Fig. 15). When a sample is irradiated with UV, it forms shallower



traps, as confirmed by the lower temperature peak of the glow curve. On heating of the UV-irradiated material, the charge carriers trapped during irradiation were released and transitioned to the conduction band. The electrons that transitioned from the conduction band were either re-trapped at the trap level or defect centre or at the hole trap or luminescence centre, where they recombine with holes, giving rise to luminescence or the glow peak. Trapped charge carriers are found inside the forbidden band gap, as confirmed by the calculated trap parameters [19, 20].

## Conclusion

$\text{Ce}^{3+}$  doped YSO phosphors ( $\text{Y}_2\text{SiO}_5:\text{Ce}^{3+}$ ) were successfully synthesized by a solid state diffusion reaction method. This method is suitable for large scale production and is eco-friendly. The sample was characterized by XRD and TL studies. From the XRD pattern, it was confirmed that the prepared phosphor had a monoclinic structure, and the particle size determined by Scherer's formula was found to be in the 20 to 50 nm range. It was also observed that there were no considerable changes in the peak position and intensity in the XRD pattern with variation of  $\text{Ce}^{3+}$  doping concentration. In the TL study, maximum peak showed general order kinetics. The general order kinetic shows formation of both deep and shallow traps for the UV-irradiated phosphor. High temperature peaks represented less fading and more stability in the present sample. Activation energy was also high for the prepared sample, ranging in between 0.7 and 1.5 eV.

## References

1. S.W.S. McKeever, *Thermoluminescence of Solids* (Cambridge University Press, New York, 1983)
2. R. Chen, S.W.S. McKeever, *Theory of Thermoluminescence Related Phenomenon* (World Scientific, Singapore, 1997), p. 29
3. C. Furetta, *Handbook of Thermoluminescence* (World Scientific, Singapore, 2003)
4. A.J.J. Bos, *Nucl. Instrum. Meth. B* **184**, 3–28 (2001)
5. N.J. Azorin, M.G. Gonzalez, C.A. Gutierrez, P.C. Salvi Roberto, *Health Phys.* **46**(2), 269–274 (1984)
6. S. Selvasekarapandian, G.M. Brahmanandhan, J. Malathi, V. Joseph, *Rad. Eff. Def. Sol.* **161–9**, 559–570 (2006)
7. J. Kaur, Y. Parganiha, V. Dubey, *Phys. Res. Int.* **2013**, 5 (2013)
8. J. Kaur, Y. Parganiha, V. Dubey, D. Singh, D. Chandrakar, *Superlattices Microstruct.* **73**, 38–53 (2014)
9. A. Twardak, P. Bilski, Y. Zorenko, T. Zorenko, V. Gorbenko, E. Mandowska, A. Mandowski, O. Sidletskiy, J. Mares, *IEEE Trans. Nucl. Sci.* **61**(1), 276 (2014)
10. T. Kärner, V. Laguta, M. Nikl, S. Zazubovich, Electron and hole traps in X-ray irradiated  $\text{Y}_2\text{SiO}_5$  and  $\text{Lu}_2\text{SiO}_5$  crystals. *Phys. Status Solidi* **251**(4), 741 (2014)
11. E. Mihokova et al., Thermally stimulated luminescence in Ce-doped yttrium oxyorthosilicate. *IEEE Trans. Nucl. Sci.* **59**(5), 2085 (2012)
12. Yogita Parganiha, Jagjeet Kaur, Vikas Dubey, K.V.R. Murthy, Near UV–blue emission from Ce doped  $\text{Y}_2\text{SiO}_5$  phosphor. *Mater. Sci. Semiconductor Process.* **31**, 715–719 (2015)
13. V. Dubey, N.S. Suryanarayana, J. Kaur, *J. Miner. Mater. Charact. Eng.* **9**(12), 1101–1111 (2010)
14. V. Dubey, J. Kaur, N.S. Suryanarayana, K.V.R. Murthy, *Res. Chem. Intermed.* (2012). doi:[10.1007/s11164-012-0872-7](https://doi.org/10.1007/s11164-012-0872-7)

15. V. Dubey, J. Kaur, S. Agrawal, N.S. Suryanarayana, K.V.R. Murthy, *Opt. Int. J. Light Electron Opt.* (2013). doi:[10.1016/j.ijleo.2013.03.153](https://doi.org/10.1016/j.ijleo.2013.03.153)
16. V. Dubey, J. Kaur, S. Agrawal, N.S. Suryanarayana, K.V.R. Murthy, *Superlattices Microstruct.* **67**, 156–171 (2014)
17. Y. Parganiha, J. Kaur, V. Dubey, D. Chandrakar, *Superlattices Microstruct.* **77**, 152–161 (2015)
18. V. Pagonis, G. Kitis, C. Furetta, *Numerical and Practical Exercises in Thermoluminescence* (Springer, New York, 2006). **ISBN-10: 0-387-26063-3**
19. R.K. Tamrakar, V. Dubey, Synthesis, structural characterization and thermoluminescence glow curve study of gadolinium-doped  $Y_2O_3$  nanophosphor. *J. Taibah Univ. Sci.* (2014). doi:[10.1016/j.jtusci.2014.11.002](https://doi.org/10.1016/j.jtusci.2014.11.002)
20. B.P. Kore, N.S. Dhoble, S.J. Dhoble, Study of anomalous emission and irradiation effect on the thermoluminescence properties of barium aluminate. *J. Lumin.* **150**, 59–67 (2015)